Computational Investigation of Thermodynamic and Mechanical Properties of B2-type CoTi Intermetallic Compound

N. Bioud[a,b],*, N. Benchiheub[c], A. Benamrani[c], M. A. Ghebouli[d,e], M. Fatmi[d],**, and Faisal Katib Alanazi[f],***

[a] *Faculty of Sciences and Technology, University of Mohamed El Bachir El Ibrahimi-Bordj Bou Arreridj, Bordj Bou Arreridj, 34000 Algeria*

[b] *Laboratory of Optoelectronic and Compounds, Faculty of Sciences, Ferhat Abbas University of Setif 1, Setif, 19000 Algeria*

[c] *Laboratory of Materials Physics, Radiation and Nanostructures (LPMRN), University of Mohamed El Bachir El Ibrahimi-Bordj BouArreridj, Bordj Bou Arreridj, 34000 Algeria*

[d] *Research Unit on Emerging Materials (RUEM), University Ferhat Abbas of Setif 1, Setif, 19000 Algeria*

[e] *Department of Chemistry, Faculty of Sciences, University of Mohamed Boudiaf, M'sila, 28000 Algeria*

[f] *Department of Physics, College of Sciences, Northern Border University, Arar, 73222 Saudi Arabia*

**e-mail: nadhira.bioud@univ-bba.dz*
***e-mail: fatmimessaoud@yahoo.fr*
****e-mail: Faisal.katib.al@gmail.com*

Abstract—This work investigates the mechanical properties of B2-type CoTi material, using the density functional theory within the pseudopotential method and a plane waves basis set as implemented in the Quantum Espresso code. Our calculation yielded values of Debye temperature $\theta_D = 414.6$ K and elastic constants $C_{11} = 226.50$ GPa, $C_{12} = 129.55$ GPa, and $C_{44} = 226.50$ GPa, respectively. To test the incertitude of calculated elastic constants C_{ij} for B2-type CoTi intermetallic compound, we compared our obtained results with the experimental values of the literature. Our findings show a good agreement with experimental data. Furthermore, using an approximation based on the quasi-harmonic model, we explore various thermodynamic properties of the B2-type CoTi intermetallic compound. The thermodynamic properties obtained in this study reveal that the free energy decreases gradually with the augmentation of the temperature, while both the heat capacity as well as the entropy increase with the raising of the temperature. At $T = 298$ K, our calculation yielded values of entropy $S = 68.35$ J mol^{-1} K^{-1} and heat capacity $C_V = 46.61$ J mol^{-1} K^{-1}, respectively. To the authors' knowledge, no previous study has reported theoretical data on the thermodynamic properties for CoTi material.

1. INTRODUCTION

Intermetallic compounds with binary constituents, as well as several ordered binary and ternary alloys, have been the subject of research for several decades [1–5]. These compounds have attracted much attention as practical materials in different technological fields [6–9]. The Co–Ti binary system includes five distinct intermetallic compounds, which are: Co$_3$Ti (L1$_2$-type), Co$_2$Ti (C36-type), Co$_2$Ti (C15-type), CoTi$_2$ (E9$_3$-type), and CoTi (B2-type) [1]. The Co–Ti system in B2-type structure exhibits several interesting mechanical properties. The elastic constants C_{ij} of the intermetallic compounds CoTi and (Co, Ni)$_3$Ti were measured experimentally using the rectangular paral-lelepiped resonance (RPR) method, and it is found that the rigidity is more pronounced in (Co, Ni)$_3$Ti than in CoTi [1]. The structural parameters, elastic stiffness constants, band structure, density of states and thermal properties of intermetallic compounds (CoTi, CoZr, and CoHf) in the B2-type are studied by an ab initio approach [8]. Liu et al. treated the effect of adding vanadium, germanium, aluminum, chromium, molybdenum, tantalum, iron, nickel and tungsten to L12 type Co$_3$Ti polycrystals having a concentration of 23 at % Ti on the mechanical properties of these alloys [10]. Their observation lies in an abnormal increase in the yield strength with the increase of temperature in the range from 473 to 973 K. A separate study was carried out by Takasugi and Izumi [11] on

Table 1. Elastic constants C_{ij} (in GPa), bulk modulus B (in GPa), C' (in GPa), and Z for B2-type CoTi along the experimental ones [1] and other theoretical values [8, 26]

Parameter	C_{11}	C_{12}	C_{44}	B	C'	Z
This work	226.50	129.55	64.69	161.87	48.48	1.33
[1]	203	129	68	154	54	1.83
[8]	286.51	113.79	74.66	171.36	86.36	0.86
[26]	261	176	99	204	43	2.29

investigating the high temperature effect on both ductility and strength of Co_3Ti-L12 type polycrystalline material. Takasugi and Izumi [11] mentioned that the yield stresses of Co_3Ti increase with temperature up to 800°C. This is consistent with previous work present in the literature, while the ultimate tensile stresses decrease monotonically with increasing temperature. Xue et al. made an elastic, electronic and thermodynamic study of binary compounds Co_2Ti and Co_2Zr at high pressure and temperature using first principles calculations [12].

Since very little is known both experimentally and theoretically about the thermodynamic properties of CoTi material, the principle of the present contribution lies in the study of thermodynamic and mechanical properties of Co−Ti in B2 phase using the projected augmented wave (PAW) pseudopotential method [13−16].

2. DESCRIPTION OF COMPUTATION METHOD

We employed in our calculations the Quantum Espresso code with thermopw tool [13−16]. The Ultra-Soft Pseudo Potentials (USPP) [17] Co_pbe_v1.2.uspp.F.UPF and ti_pbe_v1.4.uspp.F.UPF are used for cobalt (Co) and titanium (Ti) atoms, respectively. The exchange-correlation potential was *treated* using the PBE-GGA [18]. The wave functions were enlarged for the plane wave basis set with an energy cut-off of 50 Ry; however, the charge density cut-off was set at 400 Ry, resulting in a convergence with an energy threshold of 1×10^{-4} Ry. The $11 \times 11 \times 11$ k-points Monkhorst−Pack mesh was used to achieve the integration over the Brillouin zone [19]. Because the obtained values of the cut-off energy and the k-points are used in the calculation of the ground state parameters. It is noticed that the convergence tests on other physical properties are crucial to achieving a good result in the subsequent computations.

3. DISCUSSION OF RESULTS

3.1. Elastic Constants

Many fundamental solid-state properties of solids are closely related the elastic constants [20]. The number of elements decrypting the matrix of the elastic constants C depends on the symmetry of the crystal. In crystals with cubic structures, there are three independent elements in the matrix of the elastic constants, they named C_{11}, C_{12}, and C_{44} [21]. From the Quantum Espresso code, the elastic constants of B2-type CoTi were obtained using the same method used in [21]. The anisotropy factor de notedisa crucial parameter [8] in crystallography, allowing us to understand the elastic behavior of crystalline materials. In particular for cubic crystals, this factor named the Zener anisotropy factor [22−24], it is defined as follows: $Z = 2C_{44}/(C_{11} − C_{12})$ [23−25]. For completely isotropic material, Z is equal to 1, otherwise for material which is mechanically anisotropic. The bulk modulus B of cubic crystal is linearly expressed to the elastic constants C_{11} and C_{12} [25], so $B = (C_{11} + 2C_{12})/3$ [23−25]. The values of C_{11}, C_{12}, C_{44}, B, as well as those of single-crystal shear modulus C' and the elastic anisotropy factor Z of B2-type CoTi, along with their experimental ones [1] and other theoretical data [8, 26] present in the literature are listed in Table 1. The crystals with cubic structures are mechanically stable if their elastic constants stiffness C_{ij} satisfies the following conditions [25]:

$$(C_{11} + 2C_{12})/3 > 0, \quad (C_{11} - C_{12})/2 > 0, \\ C_{12} < B < C_{11}, \quad C_{44} > 0. \tag{1}$$

Our elastic constants C_{ij} calculated for B2-type CoTi material obey to these mechanical stability conditions. If C_{11} is larger than that C_{44}, the material presents a stronger resistance to the unidirectional than resistance to the pure shear deformation [25]. From Table 1, we can remark that the value (226.5 GPa) of C_{11} is larger than that (64.69 GPa) of C_{44} for CoTi intermetallic compound. It should be noted that a comparable tendency has been observed for some half-Heusler LiCaGe, LiSrGe, and LiBaGe ternary compounds [25]. We can observe also that our results of the C_{ij} are agreed well with experimental results reported by Yasuda et al. [1]. The deviations between our values of the C_{ij} and the experimental ones reported by Yasuda et al. [1] are around 10.38% for C_{11}, 0.42% for C_{12}, 5.12% for C_{44}, and 4.86% for B, respectively. On the other hand, our calculated value (1.33) of the Zener anisotropy factor Z is lower than the experimental result (1.83) reported by Yasuda et al. [1].

In single crystals, macroscopic elastic moduli like Young's modulus E, shear modulus G and Poisson ratio ν as well as wave speeds are strongly related to crystallographic direction; while in the aggregate material, all the elastic moduli arise due to an averaging over different elastic constants. As the ratio between linear stress and the corresponding strain, Young's modulus E is used to evaluate the stiffness of the solid (such as in tensile and compressive tractions testing for example). Both E and ν could deduce from B and G as follows: $E = 9BG/(3B + G)$ and $\nu = (3B - 2G)/(6B + 2G)$ [6]. The values of G, E, and ν for B2-type CoTi intermetallic compound were classified in Table 2. They are analyzed and compared with the measured values [1] and the theoretically calculated data [8]. The deviations between our values for G and E and those of Yasuda et al. [1] are around 6.3% for G and 7.47% for E, respectively.

The Cauchy pressure defined by ($Cp = C_{12} - C_{44}$) is parameter used to inform on the ductility and brittleness of a material [25]. Our achieved Cp value for CoTi intermetallic compound was also ranked in Table 2, with other data present in the literature [1, 8]. Materials with positive Cauchy's pressure $C_{12} > C_{44}$ (such as CoTi) have metallic bonds [8]. Else, it is related to the ionic character. The positive values of Cp involve that the material resists volume changes more than the changes in shape [8]. Else, it indicates that the materials more resistant to shear deformations than to volume changes. The ductile-brittle nature of the material could be estimated using two parameters; Poisson's ratio ν and Pugh's ratio (B/G). When $\nu < 0.26$, the material is brittle, otherwise it is considered as ductile. Furthermore, material with a B/G value greater than 1.75 is ductile, whereas material with a B/G value less than 1.75 is brittle [24]. Our obtained values of ν and B/G of CoTi are also classified in Table 2, along with other data from the literature [1, 8]. The value (0.34) of ν is greater than 0.26, that (2.81) of B/G is higher than 1.75, hence B2-type CoTi intermetallic compound is considered as ductile material.

The microhardness parameter is of considerable importance, thus because it characterizes the mechanical properties of solid-state surfaces [27]. This parameter is largely affected by the dislocations and other defects containing in the solid. The Vickers hardness H_V can be calculated from the formula: $H_V = 2(k^2G)^{0.585} - 3$ [28, 29], with $k = G/B$. Our result for the H_V is 3.4 GPa for CoTi intermetallic compound. No data on B2-type CoTi Vickers hardness H_V could be found in the literature to make a comparison.

To assess the machinability of CoTi intermetallic compound, a calculation using the machinability index ($\mu_M = B/C_{44}$) is performed. This index is one of the most important indicators that are used to characterize the bulk material [30], it evaluates the suitability of a material for industrial applications [29]. A good

Table 2. Mechanical moduli of CoTi, along with the experimental [1] and theoretical [8] data. Experimental result with * is obtained for ⟨100⟩ direction and not for the aggregate material

Parameter	Cp (GPa)	G (GPa)	E (GPa)	ν	B/G
This work	64.86	57.63	154.55	0.34	2.81
[1]	61	54	143	0.387*	2.85
[8]	39.13	79.13	205.74	0.29	2.16

machinability of material is marked by a combination of high tensile strength (B) to a low shear resistance (C_{44}) of the (100) plane along the [010] direction. Our calculation yields a μ_M value of approximately 2.5 for CoTi intermetallic compound. The machinability level of CoTi intermetallic compound is slightly higher than that of the perovskite $Pb(Mg_{1/3}Nb_{2/3})O_3$ substances and the MAX phases [29]. To analyze the acoustic impedance (Z) for CoTi intermetallic compound, we have used this formula: $Z = (\rho G)^{1/2}$ [31, 32]. This quantity has been found at around 19.64×10^6 Rayl, this value is of the same order of magnitude as that (19.24×10^6 Rayl) reported for Ti_2GaB material [31] and slightly higher than the result (17.88×10^6 Rayl) reported for Zr_2GaB [32], respectively.

3.2. Thermal Properties

For various solids that crystallize in a cubic phase, the melting point T_m correlates linearly with C_{11} by the following expression: T_m (K) $= 553$ (K) $+ 5.91C_{11}$ (K/GPa) [29], where the C_{11} is in GPa. The value of T_m for our material of interest; B2-type CoTi intermetallic compound is equal to 1892 K, which is larger than the value (1763 K) of Co and slightly lower than the value (2073 K) of Ti [33]. We think that there is no data on T_m exists in the literature for CoTi intermetallic compound. The Debye temperature θ_D of material is one of the interesting thermophysical parameters in solid-state physics. This quantity is directly linked to the melting temperature and specific heat [34]. Often the θ_D was deduced from the speed of the sound v_m as follows [21]:

$$\theta_D = \frac{\hbar}{k_B}\left[\left(\frac{6\pi^2 n N}{V}\right)\right]^{1/3} v_m, \qquad (2)$$

where k_B denotes the constant of Boltzmann, n denotes the number of atoms in the unit cell, $\hbar = h/2\pi$, h denotes the Planck constant and finally N denotes the number of unit cells in the volume V. The details on the determination of v_m and θ_D in cubic crystals could be found in [34, 35]. Our calculated values of the acoustic wave velocities and θ_D for B2-type CoTi were presented in Table 3, in comparison with the theoretical data of Acharya et al. [8].

Table 3. Mass density ρ, longitudinal v_l, transversal v_t, and average v_m sound velocities and Debye temperature θ_D for CoTi along other data [8]

Parameter	ρ (kg/m³)	v_l (m/s)	v_t (m/s)	v_m (m/s)	θ_D (K)
This work	6695	5971	2934	3295	414.6
[8]	5091	7377	3947	4405	314.08

One can notice that the calculated value of crystal density ρ (6.41 g/cm³) for the CoTi is comparable with the experimental result (6.41 g/cm³) [1], the percentage deviation is around 4.26%. Likewise, it is noticeable that our calculated value (414.6 K) of the θ_D for CoTi material is in good agreement, particularly with the experimental results (400 K) reported by Siethoff [2] and (387 K) reported by Wang and Luck [5], respectively. The discrepancy between the value (414.6 K) of θ_D obtained in this work and the value (400 K) measured experimentally by Siethoff [2] is only around 3.52%. Our obtained value of θ_D for B2-type CoTi is slightly lower than the values 445 K of Co and 420 K of Ti [36], respectively. Compared to the half-Heusler NiMnSb, NiMnAs, NiMnSi materials and IrMnAs compound [24], the Debye temperature θ_D of CoTi intermetallic compound is slightly higher than those of NiMnSb, NiMnAs, and IrMnAs, and it is slightly lower than that (434 K) calculated for NiMnSi, respectively [24].

We note that the value 314.08 K of θ_D obtained by Acharya et al. [8] is incorrectly calculated. If the values of ρ (5091 kg/cm³) and v_m (4405 m/s) obtained by the authors of [8] are introduced in the equation that gives θ_D, we obtain a value of around 505 K, which is much

Fig. 1. Vibrational energy U_{ph} of CoTi intermetallic compound versus temperature T.

different than that of 314.08 K reported by Acharya et al. [8].

3.3. Effect of Temperature on Thermodynamic Properties

3.3.1. Debye's vibrational energy. Because of the application of materials at elevated temperatures, it is almost always an interesting effort to investigate their behavior and the temperature dependent thermodynamic properties [37]. From the above, it is clear that there has been very little works including experimental measurements and theoretical predictions on the CoTi intermetallic compound, as well as no studies regarding its thermodynamic properties have been reported. The total internal energy of a solid is defined, in the context of the quasi-harmonic approximation, as the product of three discrete contributions: the electronic energy U_{el} resulting from the finite temperature of electrons, the ground state energy U_o and the vibrational energy U_{ph} resulting from the phonons contribution. The total intern energy can be expressed mathematically as follows for a given temperature (T) and volume (V): $U = U_{el} + U_o + U_{ph}$ [38]. According to [38], the vibrational energy is given as follows:

$$U_{ph} = \frac{1}{N}\left(\sum_{q,\eta} \frac{\hbar\omega_{q,\eta}}{2} + \sum_{q,\eta} \frac{\hbar\omega_{q,\eta}}{e^{\hbar\omega_{q,\eta}/k_B T} - 1} \right), \quad (3)$$

where $\omega_{q,\eta}$ denotes the phonon frequencies, N denotes the number of cells containing the crystal, $\hbar$ denotes the reduced Planck constant, q denotes the wave-vector, η denotes the phonon mode and k_B denotes the Boltzmann constant.

The temperature dependence of the vibrational energy U_{ph} of B2-type CoTi intermetallic compound is illustrated in Fig. 1. From 0 to 50 K, U_{ph} is nearly constant and decreases linearly with the augmentation temperature from $T > 100$ K. At temperature $T = 298$ K, the vibrational energy U_{ph} of B2-type CoTi material was found at 15.45 kJ mol⁻¹; this result is almost equal to that ~15.44 kJ mol⁻¹ estimated for B2-type YRh material [39]. We can observe that a similar qualitative behavior was reported also for PtAsP mixed pyrite phase [37] and for both mercury selenide (HgSe) and cadmium selenide (CdSe) materials in the zinc-blende phase [40].

3.3.2. Vibrational free energy. We investigate our material of interest's vibrational free energy F_{vib} further, which is provided by the following expression [38]:

$$F_{vib}(\varepsilon, T) = \frac{1}{2N} \sum_{q,\eta} \hbar\omega_\eta(q, \eta)$$
$$+ \frac{k_B T}{N} \sum_{q,\eta} \ln\left[1 - \exp\left(-\frac{\hbar\omega_\eta(q, \eta)}{k_B T} \right) \right]. \quad (4)$$
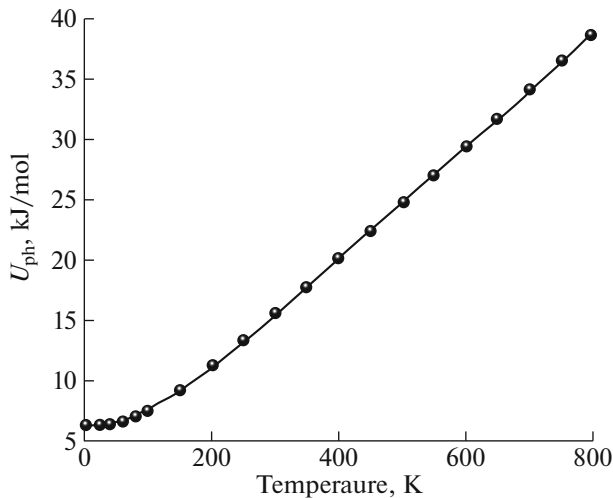
Fig. 2. Variation of the vibrational free energy F_{vib} for CoTi as a function of temperature T.

Fig. 3. Entropy S of CoTi intermetallic compound versus temperature T.

The effect of the temperature on the vibrational free energy F_{vib} for B2-type CoTi material is shown in Fig. 2. We observe that the F_{vib} regresses non-linearly with the augmentation of the temperature T. We note also that a similar qualitative behavior was observed for PtAsP material [37]. Due to the zero-point motion, values F_{vib0} and U_{ph0} are equal and do not vanish at zero-temperature [40]. For CoTi intermetallic compound, $F_{vib0} = U_{ph0} = 6.36$ kJ/mol, it is higher than the value 4.65 kJ/mol reported for YRh rare earth intermetallic compound [39] and the values 3.81 and 4.55 kJ/mol obtained for cubic zinc-blende HgSe and CdSe, respectively [40]. At $T = 298$ K, it is found at around -4.91 kJ/mol for CoTi compared to -7.40 kJ/mol for YRh material [39].

3.3.3. Vibrational entropy and constant volume heat capacity. Figure 3 displays the changes in the CoTi material's vibrational entropy S with temperature T across a range of 0 to 800 K. The entropy S of B2-type CoTi grows monotonically with temperature T. At low temperatures, it can be seen that as temperature T rises, vibrational entropy S grows swiftly. Entropy S was calculated at 298 K and found to be around 68.35 J mol^{-1} K^{-1} for the CoTi compound and 76.42 J mol^{-1} K^{-1} for YRh [39]. It should be emphasized that comparable qualitative tendencies have been documented for the cubic rock-salt scandium monophosphate (ScP) entropy S versus temperature [21].

One important characteristic that indicates a solid material's ability to store or release heat is its heat capacity [38]. Knowledge of the heat capacity of substance is essential for analyzing its vibrational properties and is vital for various industrial applications [38].
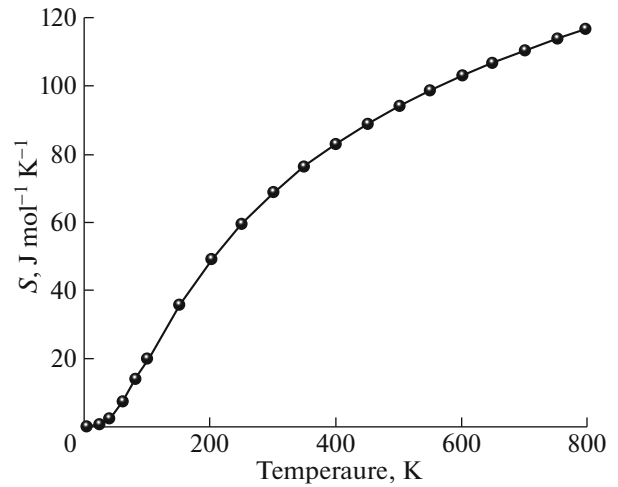
Equation (5), provides the isochoric heat capacity within the harmonic approximation.

$$C_V = \frac{k_B}{N} \sum_{qv} \left(\frac{\hbar \omega_\eta (q)}{k_B T} \right)^2 \frac{e^{\hbar \omega_\eta (q)/k_B T}}{\left(e^{\hbar \omega_\eta (q)/k_B T} - 1 \right)^2}. \qquad (5)$$

The variation of the B2-type CoTi compound's constant volume heat capacity (C_V) as a function of temperature T and pressure is shown in Fig. 4. This figure shows that, for temperatures $T < 400$ K, the C_V of CoTi increases exponentially with the augmentation of the temperature; at higher temperatures, however, it approaches the DuLong–Petit limit, which is a property shared by all solids at high temperatures [41–48], resulting from the thermal energy which sufficiently
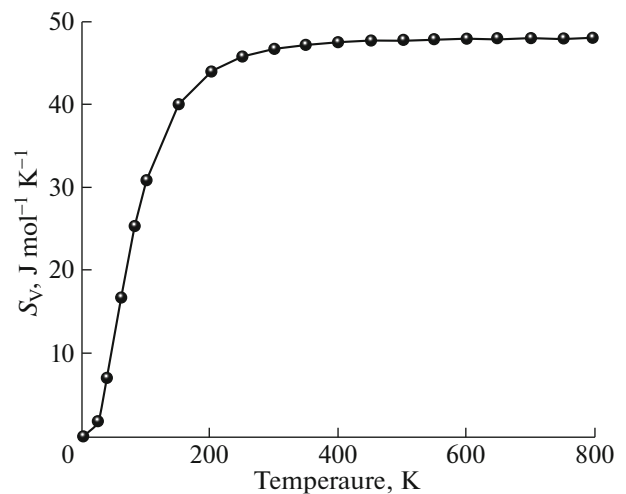

Fig. 4. Heat capacity C_V of CoTi material versus temperature T.

excites all phonon modes at high temperatures [41]. At normal temperature (298 K), the B2-type CoTi compound's C_V reached the value 46.61 J mol^{-1} K^{-1}. From the quantitative point of view, we can observe that a similar qualitative behavior for C_V versus the augmentation of the temperature was reported for PtPAs material [37], Cu_2ZnSnS_4 material [38], both mercury selenide (HgSe) and cadmium selenide (CdSe) materials in the cubic zinc-blende phase [40], molybdenum nitrides materials [43], cubic rock salt copper iodide (CuI) material [44], AsTh compound in both B1 and B2 phases [45], cubic zinc-blende silicon carbide (3C-SiC) material [47] and for aluminum phosphide (AlP) semiconductor [49, 50].

4. CONCLUSIONS

In the present work, we investigate the physical properties of B2-type CoTi material using first principal calculations; including elastic constants, elastic anisotropy factor, macroscopic elastic moduli, melting point, elastic wave speed and Debye temperature. Our calculation yielded values of Vickers hardness $H_V = 3.4$ GPa, Young's modulus $E = 154.55$ GPa and Debye temperature $\theta_D = 414.6$ K, respectively. Our data of the elastic constants and other macroscopic elastic moduli concord well with the values measured experimentally existing in the literature. For instance, our calculated values of the elastic constant C_{12}, the bulk modulus B and the Debye temperature θ_D deviate from the experimental results by only 0.42, 4.86 and 3.52%, respectively. Moreover, we explore the effect of temperature on the thermodynamic properties of our material of interest. At $T = 298$ K, our calculation yielded value heat capacity $C_V = 46.61$ J mol^{-1} K^{-1}, while at $T = 800$ K, it approaches the DuLong−Petit limit (~47.93 J mol^{-1} K^{-1}). To the best of our knowledge, this investigation presents the first analysis of the thermodynamic properties as a function of temperature T of B2-type CoTi due to the non-existence of experimental or theoretical data in the literature, which means that these first-principles predictions at high temperatures represent important new information.

AUTHOR CONTRIBUTION STATEMENT

Conceptualization: N. Bioud, Data curation: N. Ben-chiheub, Formal analysis: A. Benamrani, Methodology: M.A. Ghebouli, Validation: M. Fatmi, Faisal Katib Alanazi.

FUNDING

CONFLICT OF INTEREST

The authors of this work declare that they have no conflicts of interest.

REFERENCES

1. H. Yasuda, T. Takasugi, and M. Koiwa, Mater. Trans. JIM, **32**, 48 (1991). https://doi.org/10.2320/matertrans1989.32.48

2. H. Siethoff, Intermetallics **5**, 625 (1997). https://doi.org/10.1016/S0966-9795(97)00037-X

3. I. Hashimoto and K. Yamamoto, Philos. Mag. A **69**, 11 (1994). https://doi.org/10.1080/01418619408242206

4. U. Buchenau, H. R. Schober, J.-M. Welter, G. Arnold, and R. Wagner, Phys. Rev. B **27**, 955 (1983). https://doi.org/10.1103/PhysRevB.27.955

5. H. Wang and R. Lück, Int. J. Mater. Res. **84**, 627 (1993). https://doi.org/10.1515/ijmr-1993-840909

6. H. Rekab-Djabri, M. M. Abdus Salam, S. Daoud, M. Drief, Y. Guermit, and S. Louhibi-Fasla, J. Magnesium Alloys **8**, 1166 (2020). https://doi.org/10.1016/j.jma.2020.06.007

7. S. Daoud, N. Bioud, and P. K. Saini, J. Magnesium Alloys **7**, 335 (2019). https://doi.org/10.1016/j.jma.2019.01.006

8. N. Acharya, B. Fatima, S. S. Chouhan, and S. P. Sanya, Comput. Mater. Sci. **98**, 226 (2015). https://doi.org/10.1016/j.commatsci.2014.11.007

9. A. Benmakhlouf, A. Benmakhlouf, O. Allaoui, and S. Daoud, Chin. J. Phys. **57**, 179 (2019). https://doi.org/10.1016/j.cjph.2018.11.017

10. Y. Liu, T. Takasugi, O. Izumi, and H. Suenaga, J. Mater. Sci. **24**, 4458 (1989). https://doi.org/10.1007/BF00544530

11. T. Takasugi and O. Izumi, Acta Metal. **33**, 39 (1985). https://doi.org/10.1016/0001-6160(85)90217-2

12. M-A. Xue, X. Yuan, C. Zhong, and P. Wan, Appl. Sci. **10**, 2097 (2020). https://doi.org/10.3390/app10062097

13. P. Giannozzi, S. Baroni, N. Bonini, M. Calandra, R. Car, C. Cavazzoni, D. Ceresoli, G. L. Chiarotti, M. Cococcioni, and I. Dabo, J. Phys.: Condens. Matter **21** (39), 395502 (2009). https://doi.org/10.1088/0953-8984/21/39/395502

14. S. Baroni, A. DalCorso, S. de Gironcoli, and P. Giannozzi, Rev. Med. Phys. **73**, 515 (2001). https://doi.org/10.1103/RevModPhys.73.515

15. S. Scandolo, P. Giannozzi, C. Cavazzoni, S. de Gironcoli, A. Pasquarello, and S. Baroni, Z. Kristallogr. **220**, 574 (2005). https://doi.org/10.1524/zkri.220.5.574.65062

16. A. Dal Corso, J. Phys. Condens. Matter **28**, 075401 (2016). https://doi.org/10.1088/0953-8984/28/7/075401

17. D. Vanderbilt, Phys. Rev. B **41**, 7892 (1990). https://doi.org/10.1103/PhysRevB.41.7892

18. J. P. Perdew, K. Burke, and M. Ernzerhof, Phys. Rev. Lett. **77**, 3865 (1996). https://doi.org/10.1103/PhysRevLett.77.3865

19. H. J. Monkhorst and J. D. Pack, Phys. Rev. B **13**, 5188 (1976).
https://doi.org/10.1103/PhysRevB.13.5188

20. M. A. Ghebouli, A. Bouhemadou, B. Ghebouli, M. Fatmi, and S. Bin-Omran, Solid State Commun. **151** (14−15), 976 (2011).
https://doi.org/10.1016/j.ssc.2011.05.007

21. A. Benamrani, S. Daoud, and P. K. Saini, J. Nano-Electron. Phys. **13** (1), 01008 (2021).
https://doi.org/10.21272/jnep.13(1).01008

22. E. Tindidable, M.W. Mulwa, and B. I. Adetunji, Computational Condenced Matter **39**, e00904 (2024).
https://doi.org/10.1016/j.cocom.2024.e00904

23. E. Viswanathan, M. Sundareswari, D. S. Jayalakshmi, M. Manjula, and S. Krishnaveni, Indian J Phys. **91**, 999 (2017).
https://doi.org/10.1007/s12648-017-0996-0

24. S. Daoud, N. Bioud, N. Lebga, L. Belagraa, and R. Mezouar, Indian J. Phys. **87**, 355 (2013).
https://doi.org/10.1007/s12648-012-0231-y

25. Y. Wu, B. Wu, Z. Wei, Z. Zhou, C. F. Zhao, Y. P. Xiong, S. Tou, S. G. Yang, B. Y. Zhou, and Y. Shao, Intermetallics **53**, 26 (2014).
https://doi.org/10.1016/j.intermet.2014.04.012

26. J.-S. Zhao, Q. Gao, L. Li, H.-H. Xie, X.-R. Hu, C.-L. Xu, and J.-B. Deng, Intermetallics **89**, 65 (2017).
https://doi.org/10.1016/j.intermet.2017.04.011

27. D. Cheng, S. Zhao, and H. Ye, Philos. Mag. A **81**, 1625 (2001).
https://doi.org/10.1080/01418610108214366

28. C. Rincón and M. L. Valeri-Gil, Mater. Lett. **28**, 297 (1996).
https://doi.org/10.1016/0167-577X(96)00073-0

29. X. Q. Chen, H. Niu, D. Li, and Y. Li, Intermetallics **19**, 1275 (2011).
https://doi.org/10.1016/j.intermet.2011.03.026

30. M. A. Hadi, M. N. Islam, and M. H. Babu, Z. Naturforsch. A **74**, 71 (2019).
https://doi.org/10.1515/zna-2018-0334

31. M. F. Cover, O. Warschkow, M. M. M. Bilek, and D. R. Mckenzie, J. Phys. Condens. Matter **21**, 305403 (2009).
https://doi.org/10.1088/0953-8984/21/30/305403

32. M. Rahrah, N. Lebga, A. Latreche, S. Daoud, and A. Benmakhlouf, Ann. West Univ. Timisoara: Phys. **66**, 17 (2024).
https://doi.org/10.2478/awutp-2024-0002

33. S. Islam, M. R. Rana, K. Hoque, G. G. Biswas, M. E. Hossain, M. M. Hossain, M. M. Uddin, S. H. Naqib, and M. A. Ali, Res. Mater. **19**, 100438 (2023).
https://doi.org/10.1016/j.rinma.2023.100438

34. C. Kittel, *Introduction to Solid State Physics* (Wiley, New York, 1953).

35. M. G. Brik, J. Phys. Chem. Solids **71**, 1435 (2010).
https://doi.org/10.1016/j.jpcs.2010.07.007

36. B. Ghebouli, M. A. Ghebouli, T. Chihi, M. Fatmi, S. Boucetta, M. Reffas, Solid State Commun. **149**, 2244 (2009).
https://doi.org/10.1016/j.ssc.2009.09.001

37. S. Stølen, T. Grande, and N. L. Allan, *Chemical Thermodynamics of Materials: Macroscopic and Microscopic* (John Wiley and Sons, 2004).

38. A. I. Popoola and B. S. Agboola, Eur. J. Appl. Phys. **3**, 1 (2021).
https://doi.org/10.24018/ejphysics.2021.3.1.40

39. L. Boutahar, A. Benamrani, Z. Rouabah, and S. Daoud, Ann. West Univ. Timisoara: Phys. **65**, 160 (2023).
https://doi.org/10.2478/awutp-2023-0012.

40. A. Benamrani, S. Daoud, M. M. Abdus Salam, and H. Rekab-Djabri, Mater. Today Commun. **28**, 102529 (2021).
https://doi.org/10.1016/j.mtcomm.2021.102529

41. Y. N. Zhao, W. W. Shi, Q. Q. Zhang, J. Y. Wang, J. G. Ma, and T. Gao, Adv. Condens. Matter. Phys. **2024** (1), 5538895 (2024).
https://doi.org/10.1155/2024/5538895

42. N. Bioud, K. Kassali, and N. Bouarissa, J. Electron. Mater. **46**, 2521 (2017).
https://doi.org/10.1007/s11664-017-5335-x

43. J. Wu, J. Li, Y. Yu, and Y. Yu, CIESC J. **71**, 192 (2020).
https://doi.org/10.11949/0438-1157.20191229

44. K. Liu, B. Dong, X. L. Zhou, S. M. Wang, Y. S. Zhao, and J. Chang, J. Alloys Compd. **632**, 830 (2015).
https://doi.org/10.1016/j.jallcom.2015.01.145

45. N. Bioud, K. Kassali, X-W. Sun, T. Song, R. Khenata, S. and Bin-Omran, Mater. Chem. Phys. **203**, 362 (2018).
https://doi.org/10.1016/j.matchemphys.2017.10.016

46. Y. O. Ciftci and E. Ateser, J. Electron Mater. **49**, 2086 (2020).
https://doi.org/10.1007/s11664-019-07891-3

47. B. Ghebouli, M. A. Ghebouli, M. Fatmi, and A. Bouhemadou, Solid State Commun. **150**, 1896 (2010).
https://doi.org/10.1016/j.ssc.2010.07.041

48. S. Daoud, N. Bouarissa, H. Rekab-Djabri, and P. K. Saini, Silicon **14**, 6299 (2022).
https://doi.org/10.1007/s12633-021-01387-8

49. Y. Megdoud, R. Mahdjoubi, M. Amrani, H. Bendjeddou, S. Ghemid, H. Meradji, and R. Khenata, Comput. Condens. Matter. **22**, e00434 (2020).
https://doi.org/10.1016/j.cocom.2019.e00434

50. S. Daoud, N. Bouarissa, N. Bioud, and P. K. Saini, Chem. Phys. **525**, 110399 (2019).
https://doi.org/10.1016/j.chemphys.2019.110399